Evaluation of the Virtual Crystal Approximation

Jason M. Larkin[1] and A. J. H. McGaughey[2,*]

[1]*Department of Mechanical Engineering*

Carnegie Mellon University

Pittsburgh, PA 15213

[2]*Department of Mechanical Engineering*

Carnegie Mellon University

Pittsburgh, PA 15213

(Dated: October 9, 2012)

Abstract

I. INTRODUCTION

For thermolectric device applications, minimizing a thermoelectric material's thermal conductivity has become a promising technique for increasing $ZT > 3$.[1,2] In semiconductor alloys, understanding the effect of disorder is necessary for optimizing ZT by further lowering thermal conductivity.[3–6]

Recently, work using ab-initio calculations[7]

Abeles introduced the idea of using a virtual crystal to replace a disordered one, computing the thermal conductivity of Si/Ge alloys by treating both disorder and anharmonicity as perturbations.[8]

The goal of this work is to verify the

II. KINETIC THEORY

For a perfect system, all vibrational modes are phonons.

Diffusons, locons and propagons[9].

$$k_{vib,\mathbf{n}} = \sum_{\boldsymbol{\kappa}} \sum_{\nu} c_{ph}(\overset{\boldsymbol{\kappa}}{\nu})\, \boldsymbol{v}^2_{g,\mathbf{n}}(\overset{\boldsymbol{\kappa}}{\nu})\, \tau(\overset{\boldsymbol{\kappa}}{\nu})\,. \tag{1}$$

Here, c_{ph} is the phonon volumetric specific heat and $v_{g,\mathbf{n}}$ is the component of the group velocity vector in direction $\mathbf{n}$. Since the systems we consider are classical and obey Maxwell-Boltzmann statistics,[?] the specific heat is k_B/V per mode in the harmonic limit where V is the system volume. This approximation is used here and has been shown to be suitable for LJ argon[?] and SW silicon.[?]

Finally, we adopt the single-mode relaxation time approximation [16] as an approximate solution of the Boltzmann transport equation [17,18];

Abeles introduced the idea of using a virtual (perfect) crystal to replace a disordered one, computing the thermal conductivity of Si/Ge alloys by treating both disorder and anharmonicity as perturbations.[8]

A. Phonon Group Velocities

The group velocity vector is the gradient of the dispersion curves (i.e., $\partial\omega/\partial\boldsymbol{\kappa}$), which can be calculated from the frequencies and wavevectors using finite differences. In this work, the group velocities are calculated using finite difference and quasi-harmonic lattice dynamics because a very small finite difference can be used which reduces the error.[?]

Of particular interest if the phonon mean free path (MFP),

$$\Lambda(\substack{\boldsymbol{\kappa}\\\nu}) = |\boldsymbol{v}_g|\tau(\substack{\boldsymbol{\kappa}\\\nu}), \tag{2}$$

which requires a group velocity.

B. Phonon Lifetimes

$$\frac{1}{\tau} = \frac{1}{\tau_{p-p}} + \frac{1}{\tau_b} + \frac{1}{\tau_d}, \tag{3}$$

where τ_{p-p} accounts for phonon-phonon scattering, τ_b accounts for boundary scattering, τ_d accounts for defect scattering.

$$\tau_b = L/v_g. \tag{4}$$

Phonon-phonon scattering (τ_{p-p}) is typically treated using anharmonic perturbation theory including only 3-phonon processes.[6,7,10] At low frequencies, τ_{p-p} follows a scaling due to both normal ($B_1\omega^2$) and umklapp ($B_2\omega^2$) 3-phonon scattering processes, where the density of states is Debye-like. The constants B_1 and B_2 are typically fit to experimental data. Higher order n-phonon process can become important at higher temperatures.[10]

At low frequencies, the phonon scattering due to point-defects is given by

$$\frac{1}{\tau_d} = \frac{V\omega^4}{4\pi v_p^2 v_g}\left(\sum_i c_i(1 - m_i/\bar{m})^2 + \sum_i c_i(1 - r_i/\bar{r})^2\right), \tag{5}$$

$$\frac{1}{\tau_d} = \frac{V\omega^4}{4\pi v_p^2 v_g}\sum_i c_i(1 - m_i/\bar{m})^2, \tag{6}$$

where c_i is the fraction, m_i is the mass, and r_i is the radius (scattering cross-section) of species i and $\bar{r}$ is the average atomic radius.[11,12] The frequency dependence is the same as Rayleigh scattering, which is valid at low frequency in the Debye limit.

For all frequencies, Tamura gives a general expression for point defect scattering which is harmonic[13]

$$\frac{1}{\tau_d(\substack{\kappa \\ \nu})} = \frac{\pi}{2N}\omega_{\mathbf{q}s}^2 \sum_{\mathbf{q}'s'} \delta(\omega_{\mathbf{q}s} - \omega_{\mathbf{q}'s'}) \sum_b g(b)|e^*_{\mathbf{q}'s'}(b) \cdot e_{\mathbf{q}s}(b)|^2, \tag{7}$$

where $g(b) = \sum_i c_i(b)(1 - m_i(b)/\bar{m}(b))^2$

N is the number of unit cells.

Though the expression for harmonic scattering [Eq. (2)] is valid for small mass disorder, its use leads to good agreement with experimentally measured phonon linewidths, even in the case of the Ni0:55 Pd0:45 alloy, where the atomic species are chemically similar but mass disorder is large (mPd =mNi 14 1:812) [20].

Cahill shows that even though the mass difference between Si and Ge is larger than the mass of Si, the defect scaling agrees with experimental measurements of thermal conductivity in dilute SiGe epitaxial layers.[14]

III. VIRTUAL CRYSTAL APPROXIMATION

We calculate at all compositions the phonon modes of the virtual crystal (which has a lattice parameter, mass, and force constants of that particular composition) and derive from those the frequencies, group velocities, and lifetimes to calculate thermal conductivity.

Garg show that the virtual crystal approximation works well for Si-Ge[7]

A. Mass vs Bond Disorder

The decreased vibrational conductivity of systems which are highly anharmonic, such as weak covalently and Van der Waals bonded systems, is accounted for by the Gruneisen parameter. For a purely harmonic system, the mode specific Gruneisen parameter is zero and the phonon lifetimes are infinite.

Cahill shows that conductivty of Ge-doped Si epitaxial layers agrees with the defect scaling cross section is captured mostly by the mass disorder.[15]

The effect of bond and mass disorder has been investigated by Skye and Schelling for Si/Ge[16], where it was shown that mass disorder is the dominant scattering mechanism. Also, a first principle study of Si/Ge demonstrates that virtual crystal approxmation Marzari Si/Ge PRL[7]. A detailed study of PbTe/PbSe systems demonstrate the importance of bond environment for alloys.[?]

B. VC and Gamma DOS Comparison

Bouchard show that alloy DOS varies smoothly with concentration.[17]

C. Structure Factor of Gamma Point Modes

Demonstrates the importance of dispersion, even along different lattice directions ([100 vs [111]).

$$E^L(\substack{\boldsymbol{\kappa} \\ \nu}) = \left| \sum_{l,b} \hat{\kappa} \cdot e(\substack{\boldsymbol{\kappa} \ b \\ \nu \ \alpha}) \exp[i\boldsymbol{\kappa} \cdot \mathbf{r}_0(\substack{l \\ b})] \right|^2 \tag{8}$$

$$E^T(\substack{\boldsymbol{\kappa} \\ \nu}) = \left| \sum_{l,b} \hat{\kappa} \times e(\substack{\boldsymbol{\kappa} \ b \\ \nu \ \alpha}) \exp[i\boldsymbol{\kappa} \cdot \mathbf{r}_0(\substack{l \\ b})] \right|^2 \tag{9}$$

$$S^{L,T}(\substack{\boldsymbol{\kappa} \\ \omega}) = \sum_{\nu} E^{L,T}(\substack{\boldsymbol{\kappa} \\ \nu}) \, \delta(\omega - \omega(\substack{\boldsymbol{\kappa} \\ \nu})) \tag{10}$$

D. Group Velocity

In ordered systems, the group velocity generally scales with both the density and stiffness of the material. For example, the reduced vibrational conductivity of Ge compared to Si can be (partially) explained in both in terms of the $\bar{m}$ (germanium has a larger density ρ than silicon) and the group velocity (germanium has a smaller bulk modulus B, and $v_g \propto \sqrt{B/\rho}$. Thus, for alloys, there should also be a corrsponding scaling of the group velocity with the alloy's concentration (mass density). Duda shows the reduction in group velocity of disordered systems.[18]

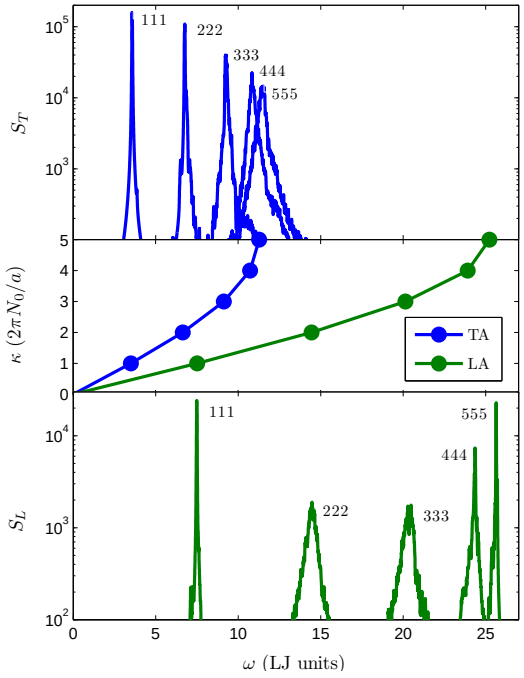

FIG. 1: virtual crystal results

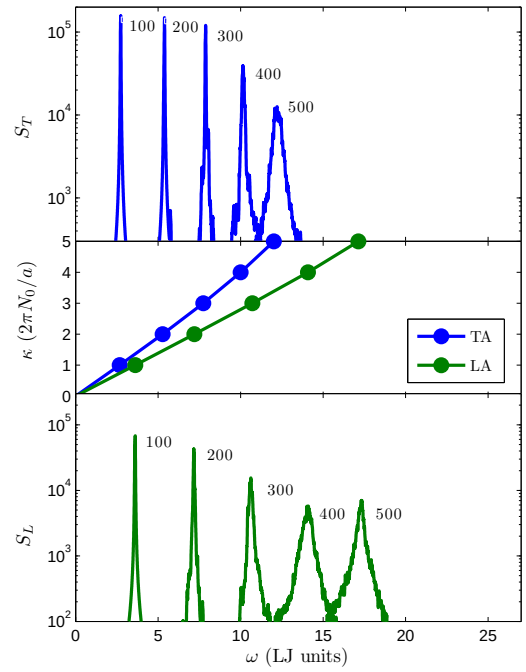

FIG. 2: virtual crystal results

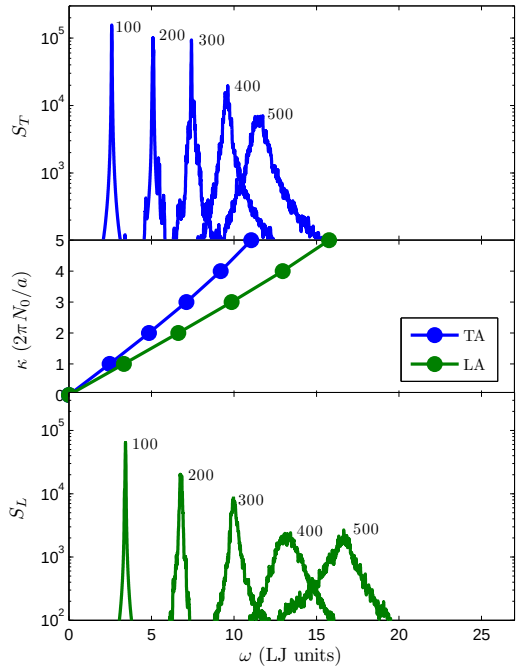

FIG. 3: virtual crystal results

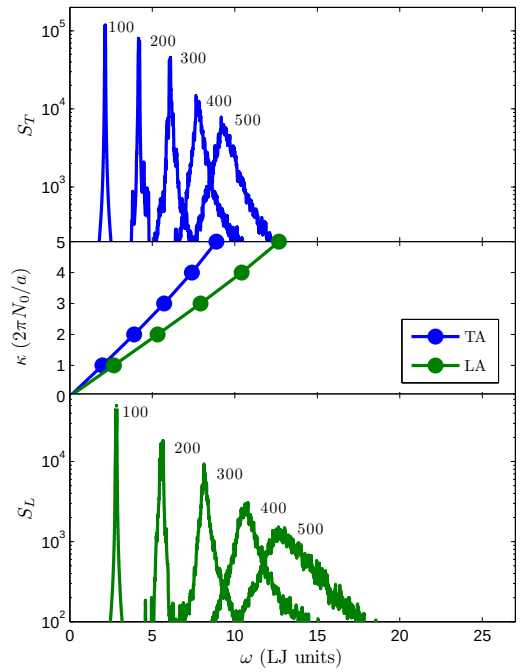

FIG. 4: virtual crystal results

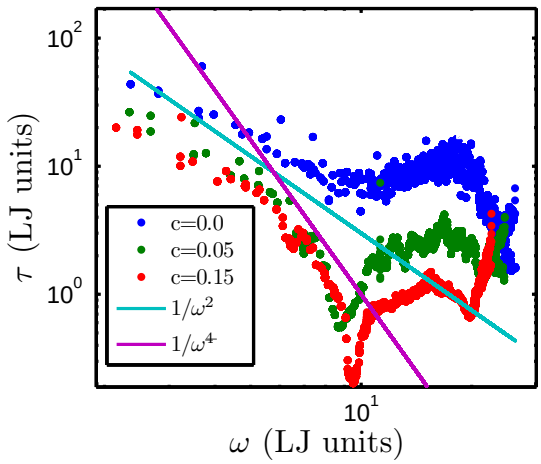

FIG. 5: virtual crystal results

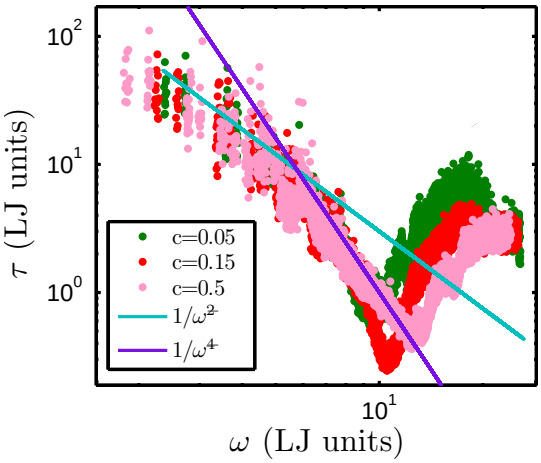

FIG. 6: gamma point results

E. VC and Gamma Point Phonon Lifetimes

IV. THERMAL CONDUCTIVITY PREDICTIONS

The thermal conductivity of amorphous solids at low temperatures contain quantum statistical effects.[19] Molecular dynamics simulations are not able to capture quantum statistical effects.

A. From Molecular Dynamics

An addition of as little as 10% Ge is sufficient to reduce the thermal conductivity to the minimum value achievable through alloying. Theoretically, mass disorder is found to increase the anharmonic scattering of phonons through a modification of their vibration eigenmodes. Notably, the thermal conductivity is found to drop sharply after only a small amount of alloying. This is due to the strong harmonic scattering of phonons even in the dilute alloy limit.

Duda shows that taking a perfect alloy and disordering via an order parameter allows control of thermal conductivity.[20]

B. From NMD and ALD using VC

C. NMD and ALD Lifetime Comparison

Essentially, the normal mode mappings are performed using eigenvectors which are plane waves.

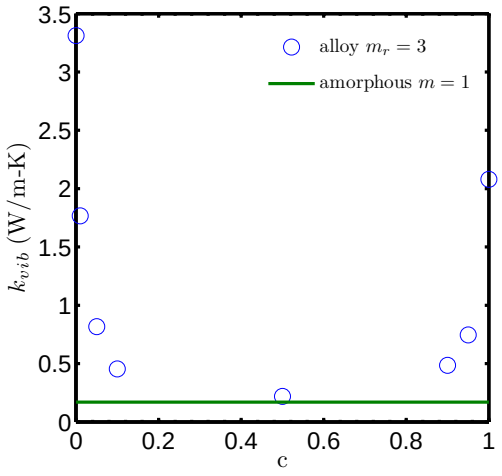

FIG. 7: The vibrational conductivity of LJ alloys predicted using MD simulations and the Green-Kubo method. The predicted thermal conductivities are for a LJ alloy of the form $m^a_{1-c}m^b_c$, where $m^a = 1$, $m^b = 3$, and $m_r = m^a/m^b = 3$ (in LJ units). As the alloy concentration is increased perturbatively, the vibrational conductivity drops quickly and saturates to a minimum at $c = 0.5$. For $c = 0.5$ the system is heavily disordered and the vibrational conductivity approaches that of an amorphous system.

V. DISCUSSION

- compare lifetimes from 2 atom alloy, 4 atom alloy. Is the reduction in thermal conductivity mostly due to the reduction in group velocities/introduction of optical modes?

A. Boundary Scattering

Boundary scattering is responsible for decreasing the long lifetimes (mean free paths) of low frequency phonons which carry a significant amount of heat, making it particularly effective at decreasing the thermal conductivity of systems with length scale of 100s of nm and less.[21]

First-principles calculations on some thermoelectric materials show that phonons have a wide MFP distribution, and hence relatively large nanostructures can reduce their lattice thermal conductivity.5,18,19 On the other hand, recent first-principles calculations have shown that the distribution is much narrower for PbTe,20 and thus, further characterizations

of the distributions and the associated detailed heat conduction of lead chalcogenides are important for better material design.

VI. SUMMARY

Appendix A: Predicted Phonon Properties: NMD vs ALD

1. Ioffe-Regel Limit on Phonon Lifetimes

For defects, the lifetimes can be reduced down to the Ioffe-Regel limit. Compare $D = v_s^2 1/\omega$ with $D = v_s a$

Appendix B: Allen-Feldman Diffuson Theory

$k_{AF} = \sum_{modes} c(\omega) D_{AF}(\omega)$

1. AF Mode Diffusivity

Shows that for c=0.5 the AF mode diffusivities agree with VC phonon mode diffusivities.

2. AF Mode Velocity

Demonstrates the importance of a mode-dependent group velocity instead of using v_s for all modes.

3. AF Thermal Conductivity Predictions

Results depend on broadening factor, except for heavily disordered systems (c=0.5 and amorphous).

4. Vibrations in Ordered and Disordered Solids

In a crystal (periodic) system, the vibrations of atoms are described by a basis of eigenfunctions called phonon normal modes, which are determined by the properties of the crys-

tal (see Appendix B 5). The eigenvalues of this basis are the phonon mode frequencies (energies).[? ?] The atomic velocities can be represented by the velocity normal mode coordinate, defined as[?]

$$\dot{u}_\alpha(\tbinom{l}{b};t) = \sum_{\boldsymbol{\kappa}',\nu}^{N,3n} \frac{1}{\sqrt{m_b N}} \exp\Big[i\boldsymbol{\kappa}' \cdot \mathbf{r}_0(\tbinom{l}{0})\Big] e^*(\tbinom{\boldsymbol{\kappa}\ b}{\nu\ \alpha})\, \dot{q}(\tbinom{\boldsymbol{\kappa}}{\nu};t)\,. \tag{B1}$$

Here, $\dot{q}(\tbinom{\boldsymbol{\kappa}}{\nu};t)$ represents the kinetic energy $T(\tbinom{\boldsymbol{\kappa}}{\nu};t)$ of the mode with phonon frequency $\omega_0(\tbinom{\boldsymbol{\kappa}}{\nu})$ by[?]

$$T(\tbinom{\boldsymbol{\kappa}}{\nu};t) = \frac{\dot{q}^*(\tbinom{\boldsymbol{\kappa}}{\nu};t)\,\dot{q}(\tbinom{\boldsymbol{\kappa}}{\nu};t)}{2}. \tag{B2}$$

The phonon mode kinetic energies $T(\tbinom{\boldsymbol{\kappa}}{\nu};t)$ are used to calculate the phonon spectral energy denisty in Appendix **??**.

5. Allowed Wavevectors in Ordered Systems

The phonon spectral energy is defined for the allowed wavevectors of a crystal, which can be specified from the crystal structure's Bravais lattice and its basis, i.e. unit cell. A D-dimensional Bravais lattice is a collection of points with positions

$$\mathbf{u}_0(\tbinom{l}{0}) = \sum_{\alpha}^{D} N_\alpha \mathbf{a}_\alpha \tag{B3}$$

where N_α and the summations if over the lattice vectors, $\mathbf{a}_\alpha$.[?] The basis (or unit cell) is the building block of the crystal and they are arranged on the points defined by the Bravais lattice. The equillibrium position of any atom in the crystal can be described by

$$\mathbf{u}_0(\tbinom{l}{b}) = \mathbf{u}_0(\tbinom{l}{0}) + \mathbf{u}_0(\tbinom{0}{b}) \tag{B4}$$

where $\mathbf{u}_0(\tbinom{l}{0})$ is the equilibrium position of the l^{th} unit cell and $\mathbf{u}_0(\tbinom{0}{b})$ is the equilibrium position of the and b^{th} atom in the unit cell relative to $\mathbf{u}_0(\tbinom{l}{0})$. For the LJ systems studied here, the cubic conventional cells are used with four atoms per unit cell.[?] For our MD simulations, cubic simulation domains with periodic boundary conditions are used with $N_1 = N_2 = N_3 = N_0$.[? ?] The allowed wavevectors for such crystal structures are

$$\boldsymbol{\kappa} = \sum_{\alpha} \mathbf{b}_\alpha \frac{n_\alpha}{N_\alpha}, \tag{B5}$$

where $\mathbf{b}_\alpha$ are the reciprocal lattice vectors[?] and $-N_\alpha/2 < n_\alpha \leq N_\alpha/2$, where n_α are integers and N_α are even integers.[?] The wavevectors are taken to be in the first Brioullin zone.[?]

FIG. 8: Thermal conductivity predictions for LJ argon calculated using phonon lifetimes predicted by Φ and Φ'.[?] (a) The finite simulation-size scaling extrapolation[? ?] is used to compare the results to bulk predictions made using the Green-Kubo method. (b) The bulk results for Φ and Green-Kubo are in good agreement temperatures of 20 and 40 K with those of other atomistic simulation methods.[?]

Allowed Wavevectors in Disordered Materials

Strictly speaking, the only allowed wavector in a disordered system is the gamma point ($\kappa = [000]$). As such, the lattice dynamics calculations are performed at the gamma point:

6. Normal Mode Decomposition

Normal mode decomposition and its limitations.[22]

If $\gamma(\overset{\kappa}{\nu}) > \omega(\overset{\kappa}{\nu})$, then the vibrational mode is overdamped. Discuss why real-space method is necessary in this case.

Appendix C: Finite Simulation-Size Scaling for Thermal Conductivity

For the LJ argon system studied in Section **??**, a finite simulation-size scaling procedure[? ?] is used to compare the thermal conductivity predictions from Φ and Φ' to those from the Green-Kubo method. The scaling procedure is demonstrated in Fig. 8. The thermal conductivity is predicted from Φ or Φ' and MD simulations with $N_0 = 4, 6, 8$, and 10. The bulk conductivity, k_∞, is then estimated by fitting the data to

$$1/k = 1/k_\infty + A/N_0, \tag{C1}$$

where A is a constant. This procedure is necessary because the first Brillouin zone is only sampled at a finite number of points for a finite simulation size, with no contribution from the volume at its center. To predict a bulk thermal conductivity, it is important to sample points near the Brillouin zone center, where the modes can have large lifetimes and group velocities.[? ?]

* Electronic address: mcgaughey@cmu.edu

[1] G. Chen, M. S. Dresselhaus, G. Dresselhaus, J.-P. Fleurial, and T. Caillat, International Materials Reviews **48**, 4566 (2003).

[2] M. Dresselhaus, G. Chen, M. Tang, R. Yang, H. Lee, D. Wang, Z. Ren, J. Fleurial, and P. Gogna, Advanced Materials **19**, 10431053 (2007), ISSN 1521-4095, URL http://dx.doi.org/10.1002/adma.200600527.

[3] T. He, J. Chen, H. D. Rosenfeld, and M. A. Subramanian, Chemistry of Materials **18**, 759762 (2006).

[4] B. Huang and M. Kaviany, Acta Materialia **58**, 4516 4526 (2010), ISSN 1359-6454, URL http://www.sciencedirect.com/science/article/pii/S1359645410002764.

[5] E. S. Toberer, A. Zevalkink, and G. J. Snyder, J. Mater. Chem. **21** (2011), URL http://dx.doi.org/10.1039/C1JM11754H.

[6] Z. Tian, J. Garg, K. Esfarjani, T. Shiga, J. Shiomi, and G. Chen, Phys. Rev. B **85**, 184303 (2012), URL http://link.aps.org/doi/10.1103/PhysRevB.85.184303.

[7] J. Garg, N. Bonini, B. Kozinsky, and N. Marzari, Phys. Rev. Lett. **106**, 045901 (2011), URL http://link.aps.org/doi/10.1103/PhysRevLett.106.045901.

[8] B. Abeles, Phys. Rev. **131**, 19061911 (1963), URL http://link.aps.org/doi/10.1103/PhysRev.131.1906.

[9] P. B. Allen, J. L. Feldman, J. Fabian, and F. Wooten, Philosophical Magazine B **79**, 1715 (1999).

[10] J. E. Turney, PhD thesis, Carnegie Mellon University, Pittsburgh, PA (2009).

[11] P. G. Klemens, Proceedings of the Physical Society. Section A **68**, 1113 (1955), URL http://stacks.iop.org/0370-1298/68/i=12/a=303.

[12] P. G. Klemens, Proceedings of the Physical Society. Section A **70**, 833 (1957), URL http://stacks.iop.org/0370-1298/70/i=11/a=407.

[13] S.-i. Tamura, Phys. Rev. B **27**, 858866 (1983), URL http://link.aps.org/doi/10.1103/PhysRevB.27.858.

[14] D. G. Cahill, F. Watanabe, A. Rockett, and C. B. Vining, Phys. Rev. B **71**, 235202 (2005), URL http://link.aps.org/doi/10.1103/PhysRevB.71.235202.

[15] D. G. Cahill and F. Watanabe, Phys. Rev. B **70**, 235322 (2004), URL http://link.aps.org/doi/10.1103/PhysRevB.70.235322.

[16] A. Skye and P. K. Schelling, Journal of Applied Physics **103**, 113524 (2008), URL http://link.aip.org/link/?JAP/103/113524/1.

[17] A. M. Bouchard, R. Biswas, W. A. Kamitakahara, G. S. Grest, and C. M. Soukoulis, Phys. Rev. B **38**, 1049910506 (1988), URL http://link.aps.org/doi/10.1103/PhysRevB.38.10499.

[18] J. C. Duda, T. S. English, D. A. Jordan, P. M. Norris, and W. A. Soffa, Journal of Physics: Condensed Matter **23**, 205401 (2011), URL http://stacks.iop.org/0953-8984/23/i=20/a=205401.

[19] J. J. Freeman and A. C. Anderson, Physical Review B **34**, 5684\textbackslash965690 (1986).

[20] J. C. Duda, T. S. English, D. A. Jordan, P. M. Norris, and W. A. Soffa, Journal of Heat Transfer **134**, 014501 (2012).

[21] A. J. H. McGaughey and A. Jain, Applied Physics Letters **100**, 061911 (2012), URL http://link.aip.org/link/?APL/100/061911/1.

[22] J. E. Turney, E. S. Landry, A. J. H. McGaughey, and C. H. Amon, Phys. Rev. B **79**, 064301 (2009), URL http://link.aps.org/doi/10.1103/PhysRevB.79.064301.